

Non-local Conductance Modulation by Molecules: STM of Substituted Styrene Heterostructures on H-Terminated Si(100)

Paul G. Piva,^{1,*} Robert A. Wolkow,^{1,†} and George Kirczenow^{2,†}

¹*National Institute for Nanotechnology, National Research Council of Canada,
Edmonton, Alberta T6G 2V4, Canada and Department of Physics,
University of Alberta, Edmonton, Alberta T6G 2J1, Canada*

²*Department of Physics, Simon Fraser University, Burnaby, British Columbia, Canada V5A 1S6*
(Dated: August 14, 2021)

One-dimensional organic heterostructures consisting of contiguous lines of CF₃- and OCH₃-substituted styrene molecules on silicon are studied by scanning tunneling microscopy and *ab initio* simulation. Dipole fields of OCH₃-styrene molecules are found to enhance conduction through molecules near OCH₃-styrene/CF₃-styrene heterojunctions. Those of CF₃-styrene depress transport through the nearby silicon. Thus choice of substituents and their attachment site on host molecules provide a means of differentially tuning molecule and substrate transport at the molecular scale.

PACS numbers: 31.70.-f, 68.37.Ef, 68.43.-h, 73.63.-b

Better understanding and control of molecule-surface interactions are key to furthering advances in catalysis research, thin film deposition and processing, chemical sensing, and molecular electronics. The scanning tunneling microscope remains an invaluable tool for studying molecule-surface interactions at the molecular scale. Its ability to probe electronic structure with sub-Angstrom resolution results from the sensitivity of tunnel current to tip-sample separation and local work function. The first STM reports of molecule-surface interactions were of localized chemical reactions with surfaces [1, 2]. On Si(111), charge distributed within the 7×7 unit cell both modulates and responds to reaction with ammonia [3]. On the unpinned n-type GaAs (110) surface, chemisorbed oxygen (being electronegative) images with increased filled-state density from transferred surface charge and induces localized surface band-bending [4]. Patterning of surface contrast by NH₃ dipole fields on GaAs has also been reported [5]. Spin flip sensitivity of adsorbates to local surface environment [6], and the effect of intermolecular interactions on surface diffusion [7] have been resolved. Underlying two dimensional electron gases [8], substrate strain [9, 10] and substrate charge transfer [11] have been found to affect adsorbate pair separation.

Observations of discrete intermolecular interactions and their effect on STM imaging contrast are limited. In cryogenic STM work, distance dependent interactions between single Au atoms were studied on NiAl[12]. One dimensional (1D) particle in a box states in Au chains on NiAl[13], and perturbation of these by physisorbed organic molecules have been reported[14, 15]. Studies of charge transfer complexes[16] and coupling between functional groups tethered to molecules are more recent[17]. STM transport in adjacent silicon atoms was found to be perturbed by dipole fields due to molecules located elsewhere in the Si 7×7 cell[18], and dipole driven ferroelectric assembly of styrene at 7K has been reported [19].

We present experimental (300 K) and theoretical re-

sults that show dipole fields produced by substituents bound to aromatic rings on styrene molecules significantly perturb transport characteristics of the host molecules, nearby molecules, and the substrate to which the molecules are attached. For one-dimensional para-substituted OCH₃-styrene/CF₃-styrene molecular heterostructures, transport through molecules at the heterojunction deviates from that of molecules elsewhere within the structure. In the case of lines of CF₃-styrene arranged *side by side*, the dipole fields increase the ionization potential of underlying silicon valence electrons.

Organic molecular heterostructures were grown using a vacuum phase self-directed growth mechanism [20] for styrene on H-terminated [21] Si(100) 2×1 surfaces[22]. Dangling bonds on the H:Si(100) surface initiate a chain reaction between surface Si atoms and styrene, leading to well ordered 1D molecular arrays along Si dimer rows. Heterostructures were formed by first dosing CF₃ (electron withdrawing) and then OCH₃ (electron donating) para-substituted styrene molecules. Such substituents are of interest as they modify the energy and spatial distribution of π and π^* states in host aromatic molecules.

Fig.1 shows the growth and bias-dependent STM imaging [23] of two CF₃-styrene/OCH₃-styrene heterowires on H:silicon. Fig.1(a) shows a 16nm \times 26nm region of the sample after a 10L (1L = 10^{-6} Torr sec) exposure of CF₃-styrene. Sample bias V_s was -3.0V. Arrows label the reactive dangling bonds at the ends of two CF₃-styrene segments where their growth terminated. Due to slight tip asymmetry, CF₃-styrene bound to either side of their host dimers image with slightly different corrugation. Comparison with images of the unreacted H:Si surface (not shown) shows the upper (lower) CF₃-styrene segments are chemically bound to the right (left) sides of their respective dimer rows. Fig.1(b) shows the same region ($V_s=-3.0V$) following a subsequent 10L exposure of OCH₃-styrene. Lines of OCH₃-styrene molecules have grown in regions marked by red rectangles, beginning at

the locations of the terminal dangling bonds of the CF₃-styrene lines in Fig.1(a). Thus two CF₃-styrene/OCH₃-styrene heterowires ('1' and '2') have been formed.

At -3.0 V, the tip Fermi-level is below the highest occupied molecular orbitals (HOMO) for the OCH₃-styrene since at this bias the tip height at constant current has saturated (see Fig.1(d)). As in our model energy level structure (inset, Fig.1(d)) at high bias the tip Fermi-level (arrow H) is below the highest OCH₃-styrene HOMO band (orange) but above the HOMO band of CF₃-styrene (violet) which therefore images lower (less bright).

Fig.1(c) shows the same region at $V_s = -1.8$ V. Here the tip Fermi-level (arrow E, Fig.1(d)) is near the top of the OCH₃-styrene HOMO band. The OCH₃-styrene continues to image above (brighter than) the CF₃-styrene, but the OCH₃-styrene molecules near the heterojunctions in heterowires 1 and 2 now image higher than those further away. The OCH₃-styrene in heterowire 1 near the terminal dangling bond also images with increased height.

Fig.1(d) presents topographic cross-sections along heterowire 1 above the trench between its attachment row (labelled with red dots in Fig.1(c)) and the vacant dimer row to its right. The topographic envelope for the heterostructure extends between ~ 1 nm and ~ 9.5 nm along

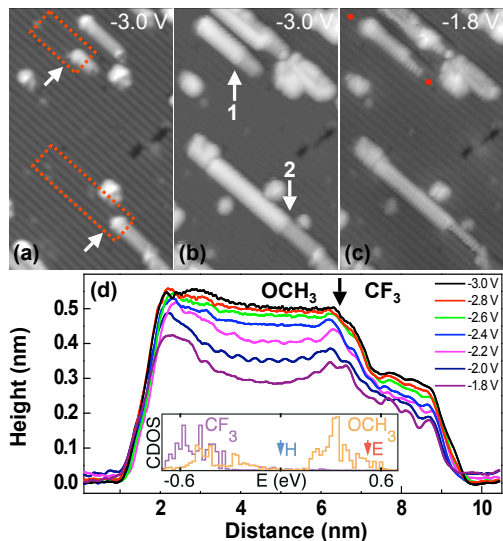


FIG. 1: Constant current filled-state STM images of CF₃-styrene/OCH₃-styrene heterowires on H:Si(100). (a) Lines of CF₃-styrene. Arrows indicate reactive dangling bonds. (b) OCH₃-styrene lines have grown in the red rectangles, extending the CF₃-styrene lines in (a) to form CF₃-styrene/OCH₃-styrene heterowires. (c): As in (b) imaged at lower bias. Molecules are bound to right side of Si dimer row marked by red dots. (d) Constant-current topographic cross-sections (0.4nm wide) of heterowire 1 along trench to right of attachment dimers. At low bias, interfacial OCH₃-styrene (black arrow) images with increased height. Tunnel current: 40pA. Inset: Molecular HOMO densities of states (C orbital projection) of OCH₃-styrene (orange) and CF₃-styrene (violet) on H:Si. Arrows H,E show STM tip E_F for plots H,E of Fig. 2.

the abscissa. The maxima associated with the terminal dangling bond and the heterojunction are at ~ 2.3 nm and ~ 6.4 nm, respectively. The sloping bias-dependent height response of the OCH₃-styrene segment near the terminal dangling bond is much like that reported in Ref. 24 for styrene: On the degenerately doped n-type H:Si surface, dangling bonds behave as acceptors, and carry negative charge. Molecular orbitals belonging to molecules in the vicinity of these charge centres are raised in energy by the localised electrostatic field. Therefore at low filled-state bias, these molecules present increased state density at the tip Fermi-level and image with increased height.

The bias-dependent height response of the OCH₃-styrene near the heterojunction is similar to that near the terminal dangling bond just described: At high bias, the interfacial OCH₃-styrene images with nearly constant height along the bulk of the homowire segment. As $|V_s|$ decreases, the height of the interfacial OCH₃-styrene (4-5 molecules closest to the heterojunction) does not decay as rapidly as in the rest of the OCH₃-styrene segment. At $V_s = -1.8$ V the interfacial OCH₃-styrene molecules image ~ 0.05 nm higher than OCH₃-styrene situated 5-7 dimers away from the heterojunction [25]. This behavior was not expected as there is no dangling bond near the junction.

STM imaging characteristics of related 1D styrene/4-methylstyrene heterostructures on (100) Si were reported in Ref. 26. No height enhancement at the heterojunction was evident in that work. The perturbation due to the methyl substituent gives rise to weaker electric dipoles than those investigated here [27]. This suggests that the height enhancement at the CF₃-styrene/OCH₃-styrene junction may be due to molecular dipoles.

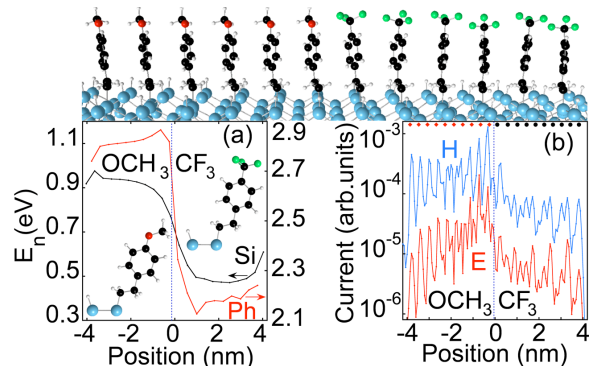


FIG. 2: (a) Calculated local electrostatic electronic energy shifts E_n vs. position in molecular chain. Red curve (Ph): Average of E_n over the benzene ring of each molecule (right scale). Black curve (Si): E_n on Si atoms to which molecules bond (left scale). (b) Calculated STM current I at low (E) and high (H) negative substrate bias vs. STM tip position along molecular chain at constant tip height. Black bullets (red diamonds) show positions of C (O) atoms of CF₃ (OCH₃) groups. Part of the heterostructure near the junction and side views of CF₃-styrene and OCH₃-styrene molecules are shown. Si,C,O,F and H atoms are blue, black, red, green and white.

To explore this possibility we carried out *ab initio* density functional calculations [28] of the electrostatic shifts $E_n = -e(W_n - U_n)$ of the local electronic energies where W_n (U_n) is the electric potential at the nucleus of atom n in the presence (absence) of all other atoms of the heterostructure. The results for a chain of 10 CF_3 -styrene and 10 OCH_3 -styrene molecules on a (100) H:Si cluster are shown in Fig.2(a); the relaxed geometry [28] of a *part* of the heterostructure near the junction is shown at the top of Fig.2. The red curve in Fig.2(a) shows E_n averaged over the aromatic ring of each molecule where most of the molecular HOMO resides; the OCH_3 -styrene (CF_3 -styrene) molecules are to the left (right) of the blue dotted line in Fig.2(a). For sterically favored orientations of the OCH_3 dipoles (negative O nearer the heterojunction than positive CH_3) the red curve rises as the junction is approached from the OCH_3 -styrene side, peaking at the 2nd OCH_3 -styrene molecule from the junction. Hence the HOMO level of this molecule is higher in energy than for any other molecule in the chain. Thus for filled state imaging, as the bias voltage $|V_s|$ increases the STM tip's Fermi level should cross the HOMO levels of the OCH_3 -styrene molecules near the heterojunction first, resulting in a pronounced low bias peak in the STM profile of the heterostructure near the heterojunction on its OCH_3 -styrene side, as is seen experimentally in Fig.1(d).

This is supported by detailed transport simulations: Extended Hückel theory tailored as in Ref. 26 to describe the band structures of Si and tungsten and the electronic structures of molecules, but modified to include the *ab initio* electrostatic energy shifts E_n [28], was used to model the electronic structure of the system. The STM current was then calculated as in Ref. 26 solving the Lippmann-Schwinger equation to determine the electron transmission probability $T(E, V_s)$ between STM tip and substrate at energy E and bias V_s . The Landauer expression $I(V_s) = \frac{2e}{h} \int_{-\infty}^{+\infty} dE T(E, V_s) (f(E, \mu_s) - f(E, \mu_d))$, where $f(E, \mu_s)$ and $f(E, \mu_d)$ are the source and drain Fermi functions, was then used to evaluate the current I .

Fig.2(b) shows the calculated STM current at constant height above the heterowire. Curve E is for a tip Fermi-level E_F just below the highest molecular HOMO state (low STM bias); see the inset, Fig.1(d). As discussed above, resonant transmission via this state (centred on the 2nd OCH_3 -styrene molecule from the junction) results in enhanced current there, consistent with experiment. Curve H shows the calculated current (at higher bias) with the tip Fermi-level below the OCH_3 -styrene HOMO band; see the inset, Fig.1(d). Here resonant tunneling occurs via the HOMO of *every* OCH_3 -styrene molecule in the array. Thus the relative interfacial current enhancement decreases as absolute current levels rise along the chain, again as in the experiment. These effects result from dipole fields due to OCH_3 substituents on the styrene molecules: Simulations with atomic positions unchanged but without electrostatic corrections remove

the interfacial current enhancement entirely. Simulations with matrix elements and basis function overlaps responsible for electronic hopping between molecules set to zero did not significantly modify the results reported here. This indicates an electrostatic origin for height enhancement at the heterojunction. Calculations with styrene replacing the CF_3 -styrene molecules confirm that the interfacial feature is mainly due to OCH_3 -styrene (rather than CF_3 -styrene) dipole fields [29].

Effects of the dipole fields are not limited to molecular energy levels: The black curve in Fig.2(a) suggests that the Si valence states may lie ~ 0.5 eV lower under the CF_3 -styrene chain than under the OCH_3 -styrene. A related heterostructure studied below highlights the response of the underlying silicon to the molecular dipole fields: Fig.3 shows STM imaging of a triple/single chain of CF_3 -styrene molecules on H:Si(100). Fig.3(a) shows a $15\text{nm} \times 10\text{nm}$ region following a 10L exposure of CF_3 -styrene ($V_s = -3.0\text{V}$). The arrow points to the reactive dangling bond at the end of the longest CF_3 -styrene line. The \star marks a short double chain of CF_3 -styrene that has grown beside the long CF_3 -styrene chain. Figs.3(b)-(d) show the same region following a 10L exposure of OCH_3 -styrene. The end of the long CF_3 -styrene chain has been extended by ~ 7 molecules of OCH_3 -styrene. Figs.3(b)

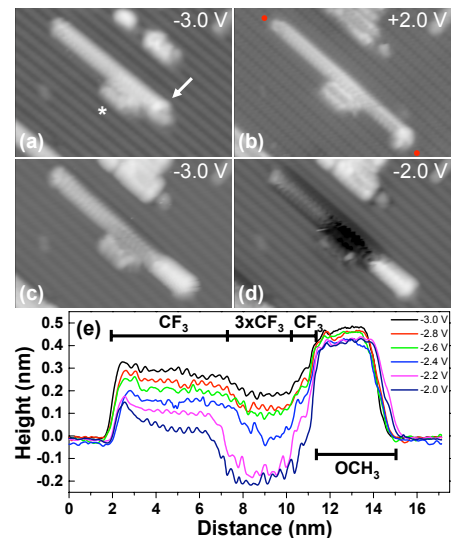


FIG. 3: STM images of a (single-triple CF_3 -styrene)/ OCH_3 -styrene heterostructure. (a) Short double CF_3 -styrene line (\star) beside longer single CF_3 -styrene chain. Arrow marks dangling bond. (b) $V_s = +2\text{V}$. Long CF_3 -styrene chain extended by ~ 7 OCH_3 -styrene molecules. (c) $V_s = -3\text{V}$. OCH_3 -styrene images above CF_3 -styrene. Single and triple CF_3 -styrene lines image with similar height. (d) $V_s = -2\text{V}$. Single OCH_3 -styrene and CF_3 -styrene lines still image above H:Si surface (brighter). Triple CF_3 -styrene chains image below H:Si surface (black). (e) Constant current topographic cross-sections (0.4nm wide) of CF_3 -styrene/ OCH_3 -styrene heterowire along trench to right of attachment dimers. Heights are relative to H:Si surface (height = 0nm). Tunnel current: 40pA.

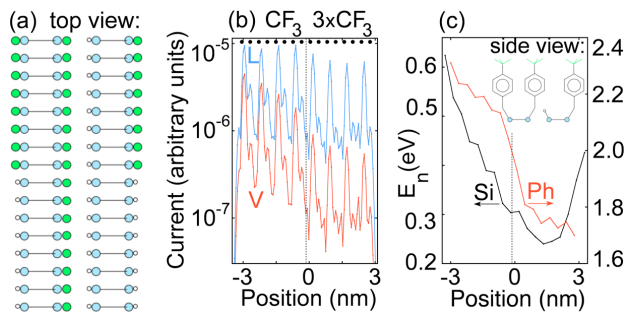


FIG. 4: (a) and inset: Schematic of model single-triple CF₃-styrene structure. (b) Calculated current profiles. Plot V: Low bias; tip Fermi level near highest Si valence band states. Plot L: Higher bias; tip Fermi level above CF₃-styrene HOMO energies. As in experiment, contrast between triple and single CF₃-styrene rows in blue profile is much weaker than in red profile. Black bullets locate C atoms of CF₃ groups. (c) Black curve: Electrostatic electronic energy shifts E_n at Si atoms to which molecules of long CF₃-styrene row bond. Triple (single) rows are right (left) of dotted line. Red curve as in Fig.2.

and (c) ($V_s = +2V$ and $-3V$, resp.) image the single and triple CF₃-styrene segments with comparable height. In Fig.3(d), V_s has been reduced to $-2.0V$ and the region with the triple CF₃-styrene lines images below (darker than) the single file chain of CF₃-styrene. Fig.3(e) shows topographic cross-sections along the CF₃-styrene/OCH₃-styrene heterowire. From $V_s = -3V$ to $V_s = -2V$, the triple CF₃-styrene chain (between 7nm and 10nm) images with decreasing height. At $V_s = -2.0V$, this region images 0.2nm below the H:Si surface indicating depleted silicon state density beneath the molecules at the tip Fermi level.

Transport simulations were undertaken for the related structure shown in Fig.4(a) (the long CF₃-styrene line is between the short ones to minimise sensitivity to cluster edges). Fig.4(b) shows the simulated constant height current along the long CF₃-styrene line. At low bias (curve V), current levels drop over the triple CF₃-styrene qualitatively as in Fig.3. The origin of this is seen in Fig.4(c): Dipole fields of the CF₃-styrene lower Si orbital energies below the triple CF₃-styrene by $\sim 0.2eV$ more than under the single file CF₃-styrene. At low bias ($V_s \sim -2.0V$) this reduced silicon state density at the tip Fermi level forces the STM tip (in experiment) to move lower over triple CF₃-styrene than over the H:Si surface to re-establish the fixed tunnel current (40 pA). It can also be concluded in this regime that lateral carrier transfer from the single chain CF₃-styrene and OCH₃-styrene regions to the triple chain CF₃-styrene region is negligible compared with the direct through-molecule transport component.

In summary, we have shown experimentally and theoretically that dipole fields established by strongly electron donating or withdrawing chemical species bound to molecules significantly modulate the transport characteristics of nearby molecules and the underlying substrate. Judicious selection of substituents attached in a site spe-

cific manner can be used to tailor electron transport at the molecular length scale and allows differential tuning of molecular vs. substrate transport characteristics.

This research was supported by CIFAR, NSERC, iCORE, Westgrid and the NRC. We have benefited from discussions with G. DiLabio and from the technical expertise of D. J. Moffatt and M. Cloutier.

* Present Address: Institute for National Measurement Standards, NRC, Ottawa, Ontario, Canada K1A 0R6.

† CIFAR Fellow, Nanoelectronics Program.

- [1] A.M. Baró, G. Binnig, H. Rohrer, Ch. Gerber, E. Stoll, A. Baratoff, F. Salvan, Phys. Rev. Lett. **52**, 1304 (1984).
- [2] R.A. Wolkow, Annu. Rev. Phys. Chem **50**, 413 (1999).
- [3] R. Wolkow, Ph. Avouris, Phys. Rev. Lett. **60**,1049(1988).
- [4] J.A. Stroscio, R.M. Feenstra, A. P. Fein, Phys. Rev. Lett. **58**, 1668 (1987).
- [5] G. Brown, M. Weimer J. Vac. Sci. Tech. B**13**,1679(1995).
- [6] A.J. Heinrich, J.A. Gupta, C.P. Lutz, D.M. Eigler, Science **306**, 466 (2004).
- [7] T. Mitsui, M.K. Rose, E. Fomin, D. F. Ogletree, M. Salmeron, Phys. Rev. Lett. **94**, 036101 (2005).
- [8] J. Repp, F. Moresco, G. Meyer, K.-H. Rieder, P. Hyldgaard, M. Persson, Phys. Rev. Lett. **85**, 2981 (2000).
- [9] R.A. Wolkow, Phys. Rev. Lett. **74**, 4448 (1995).
- [10] G.E. Thayer, N.C. Bartelt, V. Ozolins, A.K. Schmid, S. Chiang, R.Q. Hwang, Phys. Rev. Lett. **89**, 036101 (2002).
- [11] I. Fernandez-Torrente, S. Monturet, K.J. Franke, J. Fraxedas, N. Lorente, J.I. Pascual, Phys. Rev. Lett. **99**, 176103 (2007).
- [12] N. Nilius, T.M.Wallis, M. Persson, W. Ho, Phys. Rev. Lett. **90**, 196103 (2003).
- [13] T.M. Wallis, N. Nilius, W. Ho, Phys. Rev. Lett. **89**, 236802 (2002).
- [14] N. Nilius, T.M. Wallis, W. Ho, Phys. Rev. Lett. **90**, 186102 (2003).
- [15] G.V. Nazin, X. H. Qiu, W. Ho, Science **302**, 77 (2003).
- [16] F. Jäckel, U.G.E. Perera, V. Iancu, K.-F. Braun, N.Koch, J.P.Rabe, S.-W.Hla, Phys.Rev.Lett. **100**, 126102 (2008).
- [17] P.A. Lewis, C.E. Inman, F. Maya, J.M.Tour, J.E. Hutchison, P.S. Weiss, J. Am. Chem. Soc. **127**, 17421 (2005).
- [18] K.R. Harikumar, J.C. Polanyi, P.A. Sloan, S. Ayissi, W.A. Hofer, J. Am. Chem. Soc. **128**, 16791 (2006).
- [19] A.E. Baber, S.C. Jensen, E.C.H. Sykes, J. Am. Chem. Soc. **129**, 6368 (2007).
- [20] G. P. Lopinski *et al.*, Nature **406**, 48 (2000).
- [21] J. J. Boland, Surf. Sci. **261**, 17 (1992).
- [22] The Si is arsenic-doped with resistivity $< 0.005\Omega$ cm.
- [23] STM imaging was in vacuum $< 1 \times 10^{-10}$ Torr with W tips.
- [24] P. G. Piva *et al.*, Nature **435**, 658 (2005).
- [25] Heterowires were studied on multiple H:silicon surfaces with different STM tips. Additional images will be presented elsewhere[29].
- [26] G. Kirczenow *et al.*, Phys. Rev. B **72**, 245306, (2005).
- [27] A. Y. Anagaw *et al.*, J. Phys. Chem. C**112**, 3780 (2008).
- [28] Gaussian03 with the B3PW91 functional and LanL2DZ basis was used for electrostatic calculations. Gaussian98 with the UFF model was used to relax geometries.
- [29] G. Kirczenow, P. G. Piva, R. A. Wolkow, unpublished.